Supporting information for

A simple strategy for simultaneously enhancing photostability and mitochondrial-targeting stability of near-infrared fluorophores for multimodal imaging-guided photothermal therapy

Shuping Zhang, Hua Chen,* Liping Wang, Chunli Liu, Li Liu, Yu Sun and Xing-can Shen*

State Key Laboratory for Chemistry and Molecular Engineering of Medicinal Resources, School of Chemistry and Pharmaceutical Science, Guangxi Normal University, Guilin, 541004, P. R. China.

Email: chenhuagnu@gxnu.edu.cn (H. Chen)

xcshen@mailbox.gxnu.edu.cn (XC. Shen)

Table of Contents

Pages

Materials and instruments. Unless otherwise stated, all reagents were purchased from commercial suppliers and used without further purification. Solvents used were purified by standard methods prior to use. Twice-distilled water was used throughout all experiments. Mass spectra were performed using an LCQ Advantage ion trap mass spectrometer from Thermo Finnigan or Agilent 1100 HPLC/MSD spectrometer. NMR spectra were recorded on an INOVA-400 spectrometer, using TMS as an internal standard. Electronic absorption spectra were obtained on a Perkin Elmer UV Power PC spectrometer. Photoluminescent spectra were recorded at 37˚C with a HITACHI F4600 fluorescence spectrophotometer. The fluorescence imaging of cells was performed with Carl Zeiss (LSM710) confocal microscopy. The *in vivo* imaging was carried out using Bruker *In-Vivo FX PRO* system. TLC analysis was performed on silica gel plates and column chromatography was conducted over silica gel (mesh 200–300), both of which were obtained from the Qingdao Ocean Chemicals.

Determination of the fluorescence quantum yield: Fluorescence quantum yields for **AF-Cy** were determined by using ICG (Φ_f = 0.13 in DMSO) as a fluorescence standard. The quantum yield was calculated using the following equation:

$$\Phi_{F(X)} = \Phi_{F(S)} (A_S F_X / A_X F_S) (n_X / n_S)^2$$

Where Φ_F is the fluorescence quantum yield, A is the absorbance at the excitation wavelength, F is the area under the corrected emission curve, and n is the refractive index of the solvents used. Subscripts S and X refer to the standard and the test sample, respectively.

Calculation of pK_a Values. pK_a values of **AF-Cy** at acidic to near-neutral pH regions were calculated by regression analysis of the fluorescence data to fit equation (1)

$$pH - pK_a = \log (F_{max} - F)/(F - F_{min}) \qquad (1)$$

Where F is the area under the corrected emission curve, F_{max} and F_{min} are maximum and minimum limiting values of F, respectively.

Cell culture.

The mouse fibroblasts L929 and B16 cells were cultured in DMEM (Gibco, USA) supplemented with 10 % heat-inactivated fetal bovine serum (FBS), streptomycin

(100 mg mL^{-1}) and penicillin (100 units mL^{-1}). The same condition was maintained for HeLa human cervical cancer cells and 4T1 mouse breast tumor cells were cultured in RPMI 1640 (Gibco, USA). Both All the cell lines were obtained from the Shanghai Institute of Cells (Chinese Academy of Sciences), and cultured at 37 °C in a humidified atmosphere with 5 % CO_2.

Cell Viability Assay.

L929, Hela, B16 and 4T1 cells were seeded in a 96-well plate at a density of 1×10^5 cells per well and incubated for 24 h. After this initial incubation period, different concentrations of **AF-Cy** were added and the cells were incubated for 24 hours. The medium was then removed and replaced with 10 μL MTT solution (0.5 mg mL^{-1} in PBS) and incubated for another 4 h. After MTT incubation, the medium was replaced with 100 μL DMSO per well to solubilize the formazan. Formazan concentration was determined by measurement of 580 nm absorbance using a microplate reader. For phototoxicity test, Hela and 4T1 cells were incubated with 15 μM **AF-Cy** and **Cy**. And then Cells were washed with PBS and irradiated using a 638 nm laser 1.0 W cm^{-2} for 5 min. Finally, the cells were cultured for an additional 24 h and in vitro cytotoxicity was assessed by standard MTT assay.

Live/Dead Cell Assay.

4T1 cells were used to further investigate the targeted cell killing ability of **AF-Cy** and **Cy**. Cells were seeded at a density of 5×10^4 cells per well in a 6-well plate and cultured at 37 °C for 5% CO_2 for 24 h. Cells were incubated with **AF-Cy** and **Cy** at a concentration of 15 μM for 12 hours. After irradiation with 638 nm laser (1.0 W cm^{-2}) for 5 min, cells were stained with calcein acetoxymethyl (AM) ester and

propidium iodide (PI) staining reagents for 15 minutes. And then cells were washed in PBS to remove excess staining reagents.

Mitochondrial localization.

4T1 cells and HeLa cells in the exponential phase of growth on 35-mm glass-bottom culture dishes (Φ35 mm) for 24 h to reach 50-60% confluency. These cells were used in co-localization experimentation. The cells were washed three times with PBS, and then incubated with 1 mL RPMI-1640 containing various commercially available organelle-selective trackers in an atmosphere of 95 % air with 5 % CO_2 for 30 min at 37 ℃. Wash cells thrice with PBS at room temperature and then add 1mL RPMI-1640 culture medium containing 5 μM **AF-Cy** at 37 ℃ in 95 % air with 5 % CO_2 for 30 min. The cells were washed three times with PBS and observed under a confocal microscopy (LSM710, Zeiss).

CCCP (m-chlorophenyl hydrazone) treatment.

4T1 cells and HeLa cells were separately pretreated with media containing **AF-Cy**, **Cy** (5.0 μM each) for 5 h. The media were replaced with PBS containing CCCP (10.0 μM) and incubated for either 1 h or 3 h at 37 °C. The cells were washed three times with PBS. Fluorescent confocal images were then recorded using excitation wavelengths of 633 nm, and band-path emission filters at 643-754 nm.

Model protein fixability of AF-Cy.

BSA (80 μL, 1μg/L) was treated with **Cy**, **AF-Cy-2** or **AF-Cy-3** (5 μL, 1mM) at 37 °C for 5 h. The sample was used for SDS-PAGE (sodium dodecyl sulfate-polyacrylamide gel electrophoresis) on a 4-20% gradient Novex Tris-Glycine gel (Invitrogen, Carlsbad, CA, USA) followed by staining with GelCode Blue Stain Reagent (Pierce, Rockford, IL) and analysis under Gel imager.

In vivo photothermal therapy of AF-Cy.

Female Balb/c mice (weight ≈ 18 g) were obtained from Hunan Slack Jingda Experimental Animal Co., Ltd. Mouse breast cancer cells (4T1 cells) were injected into mice to form subcutaneous breast tumors. 4T1 cells were cultured to an optimal

density, digested with trypsin and then washed with PBS to form a cell suspension of 10×10^7 cells mL^{-1}. 100 μL of this suspension (5×10^6 cells) was injected subcutaneously in the right posterior of each Balb/c mouse. After a week, tumors reached approximately 100 cm^3 and were used in the following experiments. The mice were randomly divided into six groups (five mice for each group) to accept different treatments. Animals bearing implanted tumors were treated with **AF-Cy**, **Cy**, saline (100 μM). The treated mice were exposed to 638 nm laser of 1 W cm^{-2} for 5 min of **AF-Cy**, **Cy** or saline at the post-injection time of 10 min. IR thermal camera was used to monitor and record the temperature change of the tumor during irradiation. The tumor volumes were measured in two dimensions using a slide caliper and calculated as $V = a \times b^2 / 2$ (a and b: the longest and shortest diameter of tumor respectively). At the end of the administrations, mice were sacrificed, and the tumors and major organs (including heart, liver, spleen, lung and kidney) were excised, weighed and sectioned for pathological analysis. The tissues were fixed with 10% formalin and embedded in paraffin for histological analysis using haematoxylin-eosin (H&E) stains.

Fluorescence imaging in living Mice.

Tumor-bearing mice (3-4weeks old) were divided into two groups. One group was given post-injection with **AF-Cy** (100 μM, in 20 μL DMSO). The second group was given post-injection with **Cy** (100 μM, in 20 μL DMSO). After the **AF-Cy** and **Cy** post-injection, the mice were imaged using a Kodak in vivo FX Pro imaging system (Bruker).

Phantom optoacoustic imaging.

Phantom optoacoustic imaging was conducted with MSOT system (in Vision 128, iThera Medical GmbH). The test solutions containing different concentrations of **AF-Cy** (5, 10, 20, 30, 40, 50 μM) then added into commercial Wilmad NMR tubes for phantom optoacoustic imaging at room temperature.

Animal optoacoustic imaging.

4T1 tumor bearing mice were given a post-injection of **AF-Cy** (100μM). Then, the mice were anesthetized with continuous isofurane and placed in the prone position in

animal holder for imaging at 30 min. A multispectral optoacoustic tomography scanner was used to acquire the PA images at 700 nm. Cross-sectional images were acquired from the tumor regions with a step size of 0.5 mm.

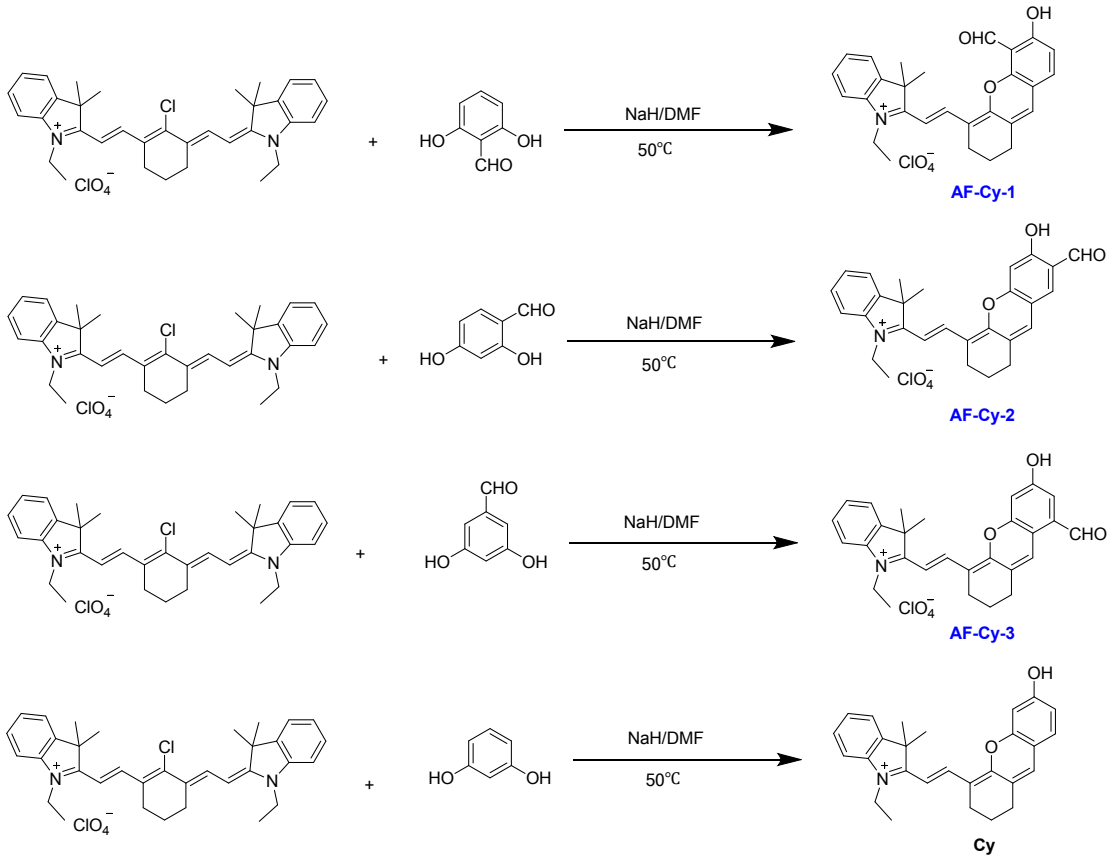

Scheme S1. Synthesis of compounds **AF-Cy-1–3** and **Cy** without aldehyde group.

Synthesis of compound AF-Cy-1.

The chloro-substituted cyanine (100.0 mg, 0.16 mmol) and NaH (60% in mineral oil, 8 mg, 0.33 mmol) were placed in a flask containing DMF (2 mL), and the mixture was stirred at room temperature under nitrogen atmosphere for 10 min. 2,6-dihydroxybenzaldehyde (44 mg, 0.32 mmol) in DMF (1.0 mL) was introduced to the mixture via a syringe, and the reaction mixture was heated at 50 °C for 2 h. The solution was then removed under reduced pressure. The crude product was purified by silica gel flash chromatography using CH_2Cl_2/ EtOH (20: 1) as eluent to give **AF-Cy-1** as a blue-green solid (32 mg, yield 38.0%). ^{1}H NMR (600 MHz, $CDCl_3$) δ 10.72 (s,

1H), 8.62 (d, *J* = 13.5 Hz, 1H), 7.55 (d, *J* = 8.4 Hz, 1H), 7.53-7.51 (m, 1H), 7.49- 7.46 (m, 1H), 7.43 (d, *J* = 7.8 Hz, 1H), 7.15 (dd, *J* = 8.6, 2.4 Hz, 1H), 7.07 (s, 1H), 6.95 (d, *J* = 8.6 Hz, 1H), 6.72 (d, *J* = 13.9 Hz, 1H), 4.56 (2H), 2.87 (2H), 2.76 (2H), 2.00 (2H), 1.83 (6H), 1.59 (3H). ^{13}C NMR (150 MHz, $CDCl_3$) δ 190.32, 177.50, 164.87, 159.16, 154.75, 145.56, 142.27, 140.91, 135.73, 131.09, 129.46, 128.68, 128.01, 122.50, 116.08, 115.28, 114.33, 113.02, 108.97, 106.30, 50.89, 41.66, 31.46, 29.73, 28.05, 22.73, 20.17, 14.17. HRMS (ESI) m/z calcd for $C_{28}H_{28}NO_3^+$ (M^+) 426.2064, Found: 426.2062.

Synthesis of compound AF-Cy-2.

The chloro-substituted cyanine (100.0 mg, 0.16 mmol) and NaH (60% in mineral oil, 8 mg, 0.33 mmol) were placed in a flask containing DMF (2 mL), and the mixture was stirred at room temperature under nitrogen atmosphere for 10 min. 2,4-dihydroxybenzaldehyde (43.2 mg, 0.32 mmol) in DMF (1.0 mL) was introduced to the mixture via a syringe, and the reaction mixture was heated at 50 °C for 2 h. The solution was then removed under reduced pressure. The crude product was purified by silica gel flash chromatography using CH_2Cl_2/ EtOH (20: 1) as eluent to give **AF-Cy-2** as a blue-green solid (29 mg, yield 35.0%). ^{1}H NMR (500 MHz, $CDCl_3$) δ 9.92 (s, 1H), 8.64 (d, *J* = 15.3 Hz, 1H), 7.70 (s, 1H), 7.53 (d, *J* = 6.9 Hz, 2H), 7.46 (dd, *J* = 16.6, 7.7 Hz, 2H), 7.09 (s, 1H), 6.81 (s, 1H), 6.69 (d, *J* = 15.2 Hz, 1H), 4.54 (q, *J* = 7.3 Hz, 2H), 2.79-2.70 (m, 4H), 1.97-1.93 (m, 2H), 1.80 (s, 6H), 1.57 (t, *J* = 7.3 Hz, 3H). ^{13}C NMR (125 MHz, $CDCl_3$) δ 194.81, 178.40, 164.25, 158.62, 157.88, 146.40, 142.35, 140.75, 133.13, 129.42, 128.21, 122.53, 118.65, 116.26, 115.60, 113.17, 106.72, 103.70, 51.18, 41.54, 29.64, 29.19, 27.82, 23.92, 20.18, 13.11. HRMS (ESI) m/z calcd for $C_{28}H_{28}NO_3^+$ (M^+) 426.2064, Found: 426.2059.

Synthesis of compound AF-Cy-3.

The chloro-substituted cyanine (100.0 mg, 0.16 mmol) and NaH (60% in mineral oil, 8 mg, 0.33 mmol) were placed in a flask containing DMF (2 mL), and the mixture was stirred at room temperature under nitrogen atmosphere for 10 min. 3,5-dihydroxybenzaldehyde (43.2 mg, 0.32 mmol) in DMF (1.0 mL) was introduced to the mixture via a syringe, and the reaction mixture was heated at 50 °C for 2 h. The solution was then removed under reduced pressure. The crude product was purified by silica gel flash chromatography using CH_2Cl_2/EtOH (20: 1) as eluent to give compound **AF-Cy-3** as a blue-green solid (35 mg, yield 41.0%).^{1}H NMR (500 MHz, DMSO-d_6) δ 10.22 (s, 1H), 8.56 (d, J = 15.1 Hz, 1H), 8.26 (s, 1H), 7.79 (d, J = 7.2 Hz, 1H), 7.72 (d, J = 8.0 Hz, 1H), 7.56 (t, J = 7.3 Hz, 1H), 7.48 (t, J = 7.4 Hz, 1H), 7.34 (d, J = 2.4 Hz, 1H), 7.17 (d, J = 2.2 Hz, 1H), 6.61 (d, J = 15.1 Hz, 1H), 4.46 (q, J = 7.2 Hz, 2H), 2.73 (dt, J = 32.1, 5.8 Hz, 4H), 1.87-1.81 (m, 2H), 1.76 (s, 6H), 1.39 (t, J = 7.2 Hz, 3H). ^{13}C NMR (125 MHz, DMSO) δ 193.21, 177.66, 174.83, 159.52, 154.86, 145.19, 142.76, 141.46, 132.26, 130.11, 127.74, 123.32, 119.12, 114.55, 113.66, 107.68, 105.35, 70.24, 51.02, 35.58, 31.74, 29.48, 27.67, 22.55, 20.40, 14.41, 13.20. HRMS (ESI) m/z calcd for $C_{28}H_{28}NO_3^+$ (M^+) 426.2064, Found: 426.2051.

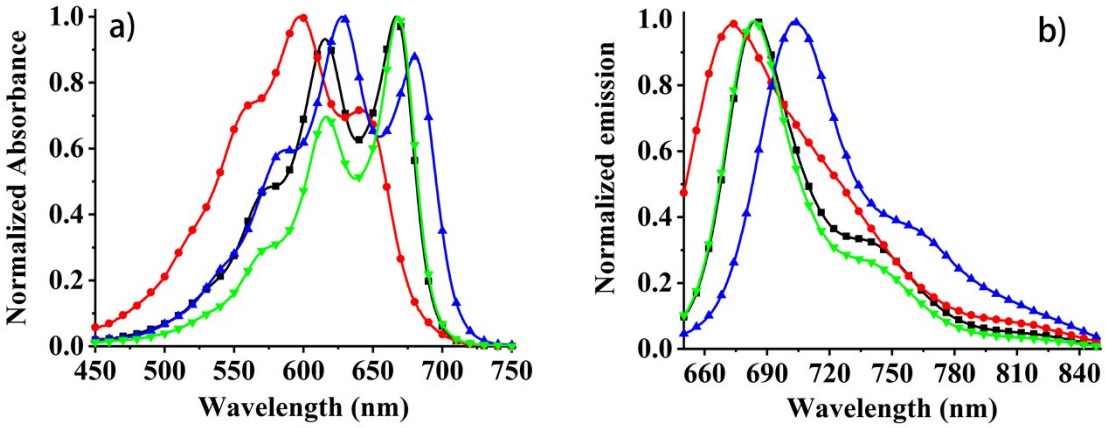

Figure S1. Normalized absorption (a) and fluorescence emission (b) spectra of 5 μM compounds **AF-Cy-1** (■), **AF-Cy-2** (●), **AF-Cy-3** (▲), **Cy** (▼) in DCM.

Table S1. Photophysical data of **AF-Cy-1–3** dyes in DCM.

Compd.	λ_{max} (nm)	ε_{max}(10^4 M^{-1} cm^{-1})	λ_{em} (nm)	Φ	Stokes Shifts (nm)
AF-Cy-1	615/664	5.9/6.4	684	0.04	69
AF-Cy-2	600	3.7	674	0.02	74
AF-Cy-3	627/680	4.3/3.7	703	0.02	76
Cy	667	6.6	683	0.08	16

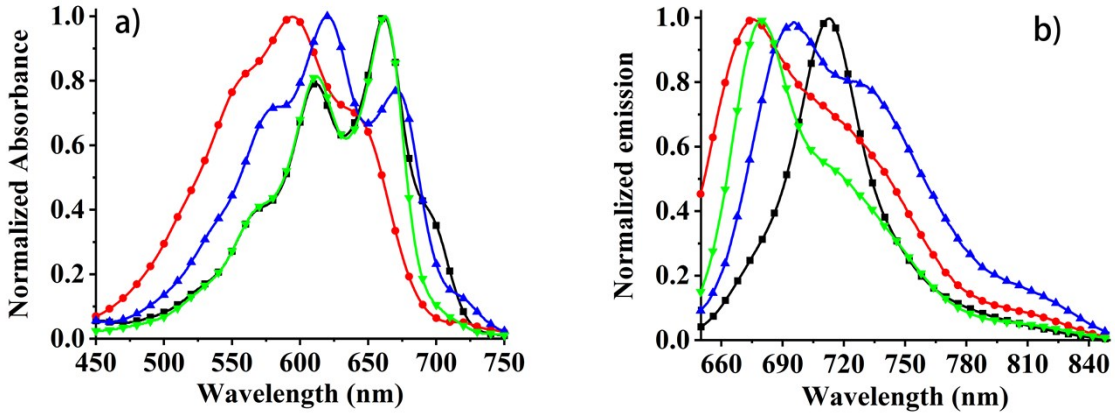

Figure S2.Normalized absorption (a) and fluorescence emission (b) spectra of 5 μM compounds **AF-Cy-1** (■), **AF-Cy-2** (●), **AF-Cy-3** (▲), **Cy** (▼) in EtOH.

Table S2. Photophysical data of **AF-Cy-1–3** dyes in EtOH.

Compd.	λ_{max} (nm)[a]	ε_{max}(10^4 M^{-1} cm^{-1})	λ_{em} (nm)[b]	Φ	Stokes Shifts (nm)
AF-Cy-1	661	4.9	712	0.46	51
AF-Cy-2	596	3.4	675	0.28	79
AF-Cy-3	620	3.3	697	0.24	77
Cy	662	3.7	680	0.29	18

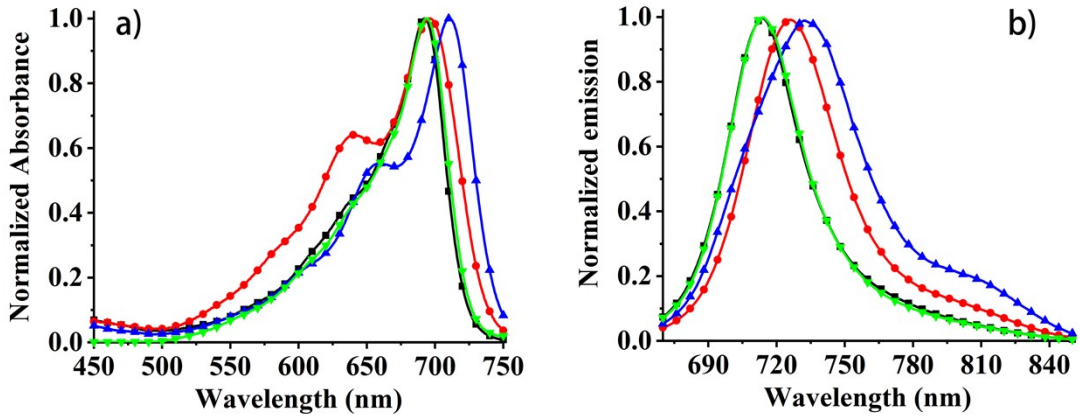

Figure S3. Normalized absorption (a) and fluorescence emission (b) spectra of 5 μM compounds **AF-Cy-1** (■), **AF-Cy-2** (●), **AF-Cy-3** (▲), **Cy** (▼) in PBS.

Table S3. Photophysical data of **AF-Cy-1–3** dyes in PBS.

Compd.	λ_{max} (nm)[a]	ε_{max}(10^4 M^{-1} cm^{-1})	λ_{em} (nm)[b]	Φ	Stokes Shifts (nm)
AF-Cy-1	692	6.9	712	0.19	20
AF-Cy-2	696	4.9	725	0.15	29
AF-Cy-3	710	5.1	733	0.16	23
Cy	693	6.3	714	0.20	21

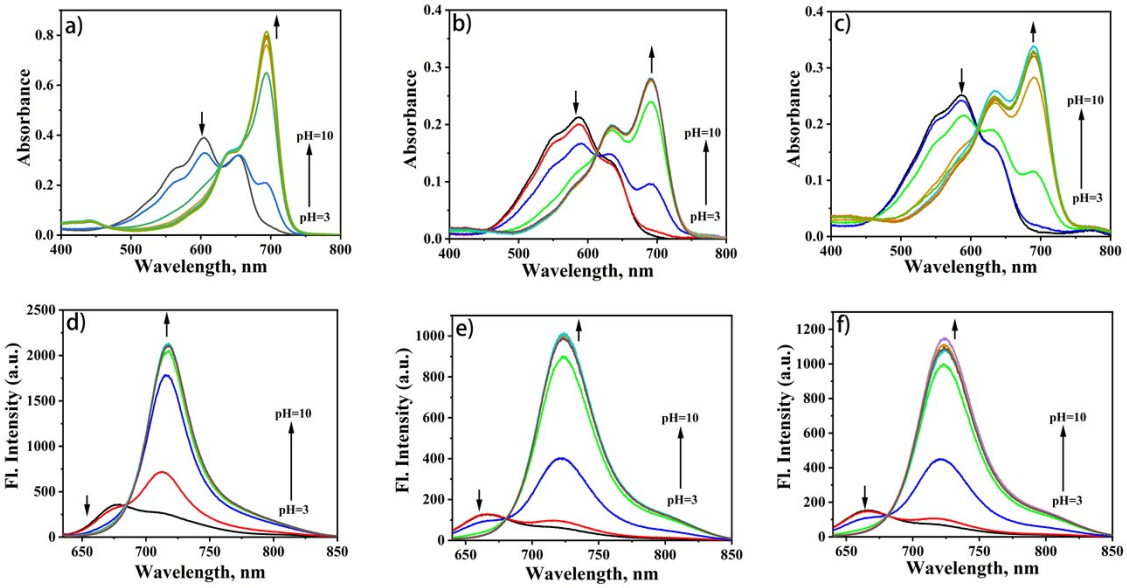

Figure S4. pH-dependence of the absorption and emission spectra of compound **AF-Cy-1–3** with the arrows indicating the change of the absorption and emission intensities with pH enhancement from 3 to 10. (a) the absorption of **AF-Cy-1**; (b) the absorption of **AF-Cy-2**; (c) the absorption of **AF-Cy-3**; (d) the emission of **AF-Cy-1**; (e) the emission of **AF-Cy-2**; (f) the emission of **AF-Cy-3**.

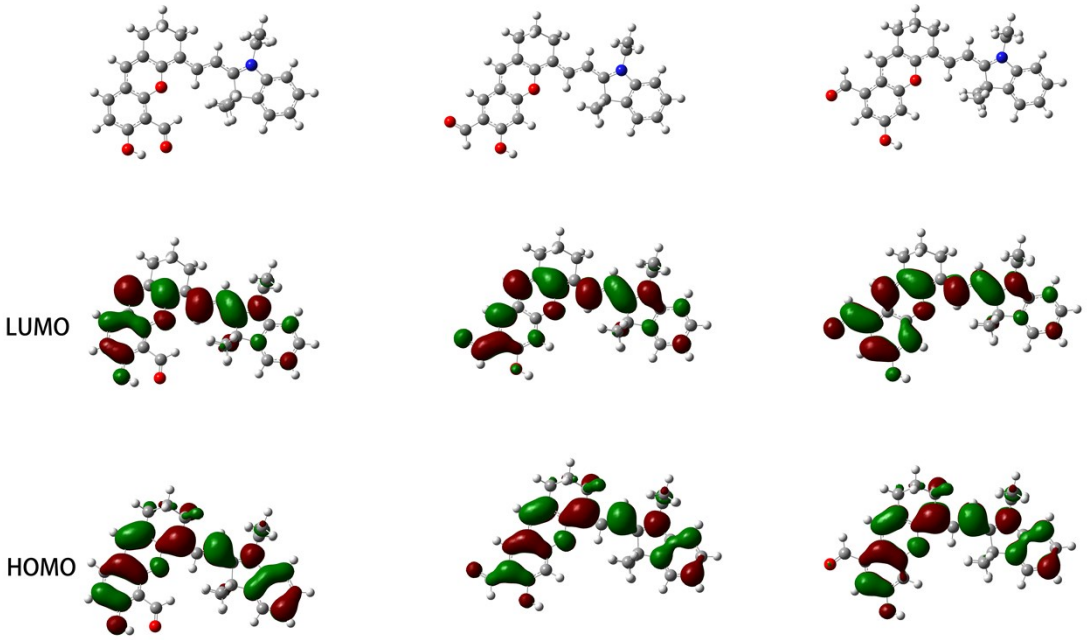

Figure S5. DFT optimized structures, the electron-density distribution of LUMO and HOMO in **AF-Cy-1–3** based on 6-31G(d) basis sets in Gaussian 09 programs.

Carbon, nitrogen and oxygen atoms are colored in gray, blue and red, respectively.

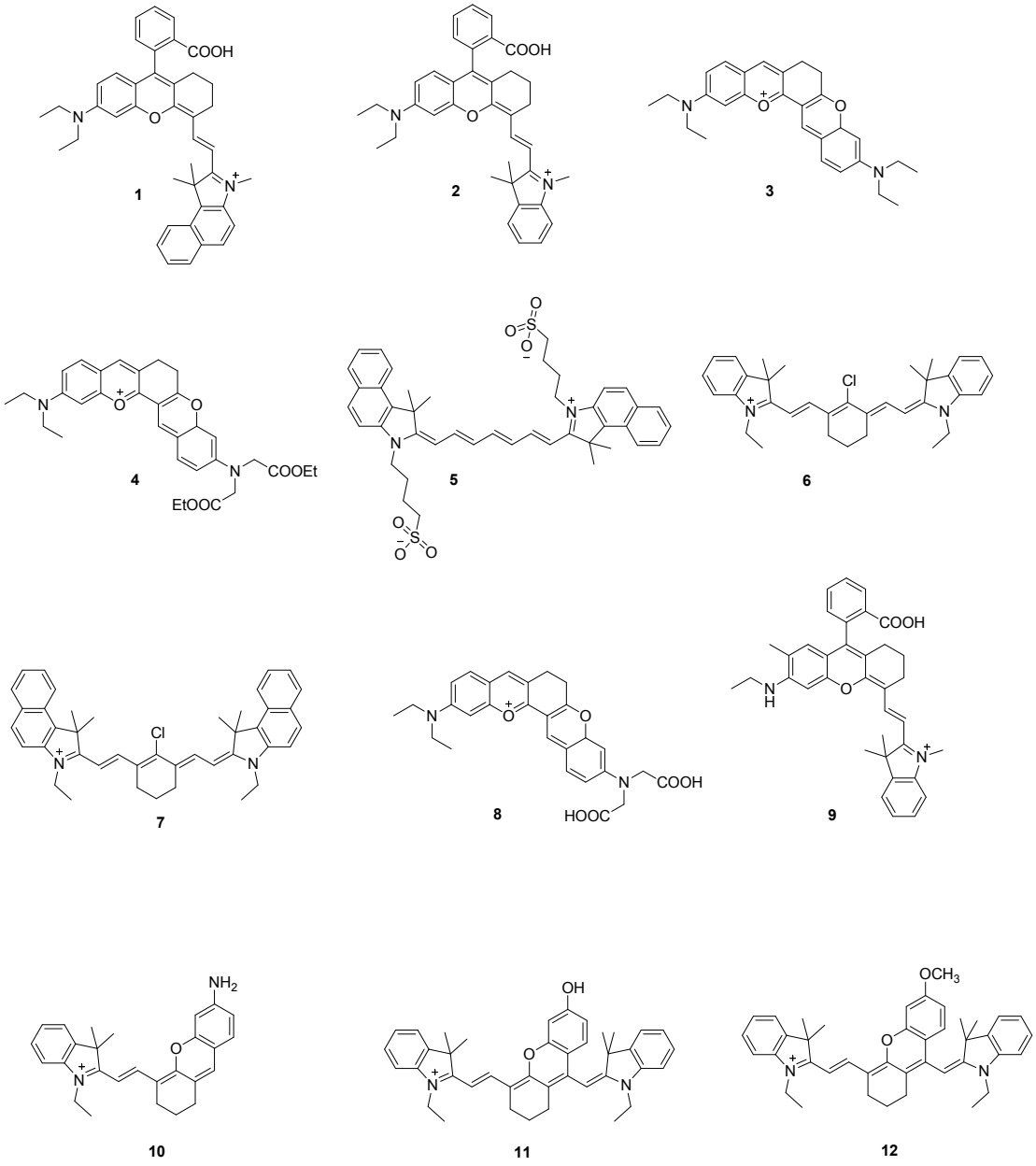

Scheme S2. Structures of compounds **1-12**.

.

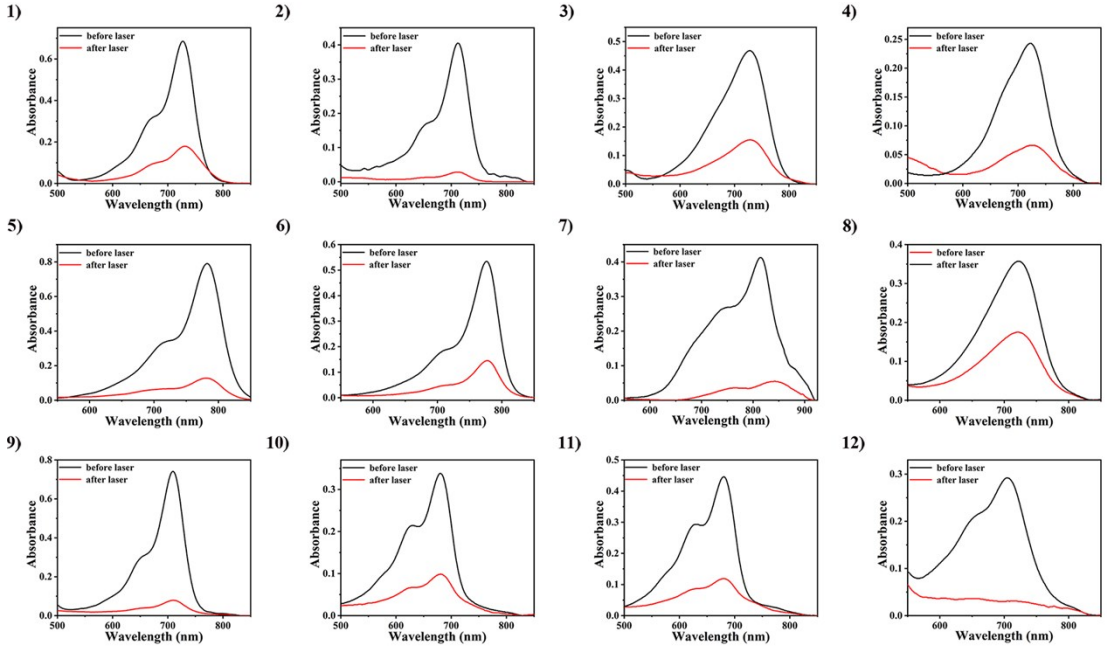

Figure S6. The absorption spectra of compounds **1-12** before and after irradiation by 638 nm(1 W/cm^2） laser for 8 min.

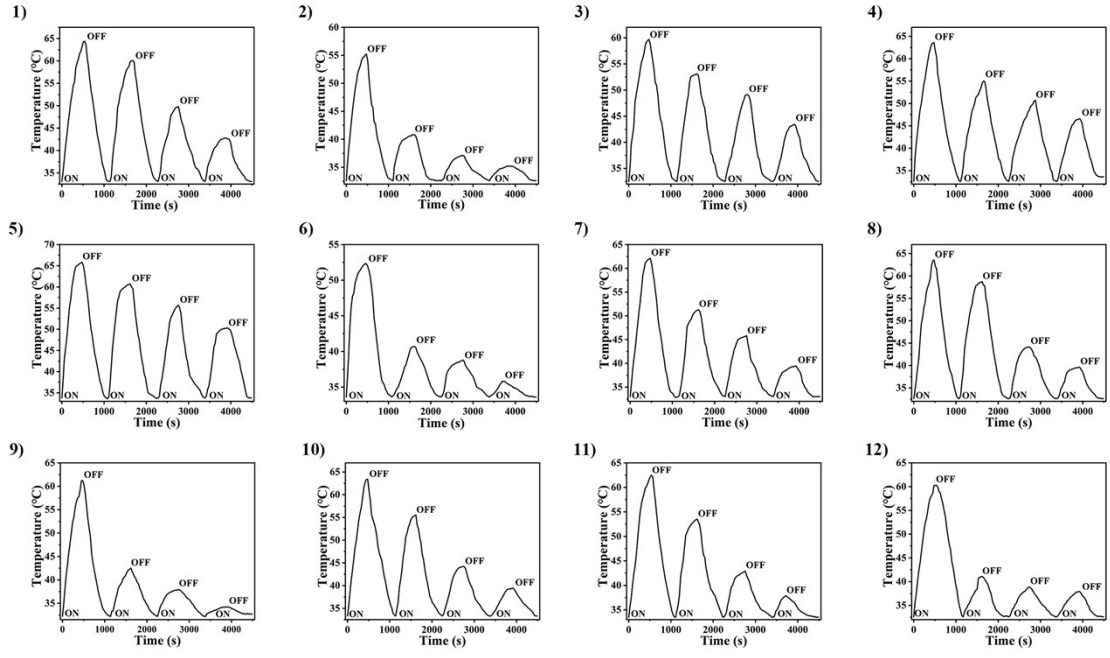

Figure S7. Photothermal cycling test of compounds **1-12** irradiation by 638 nm(1 W/cm^2) laser.

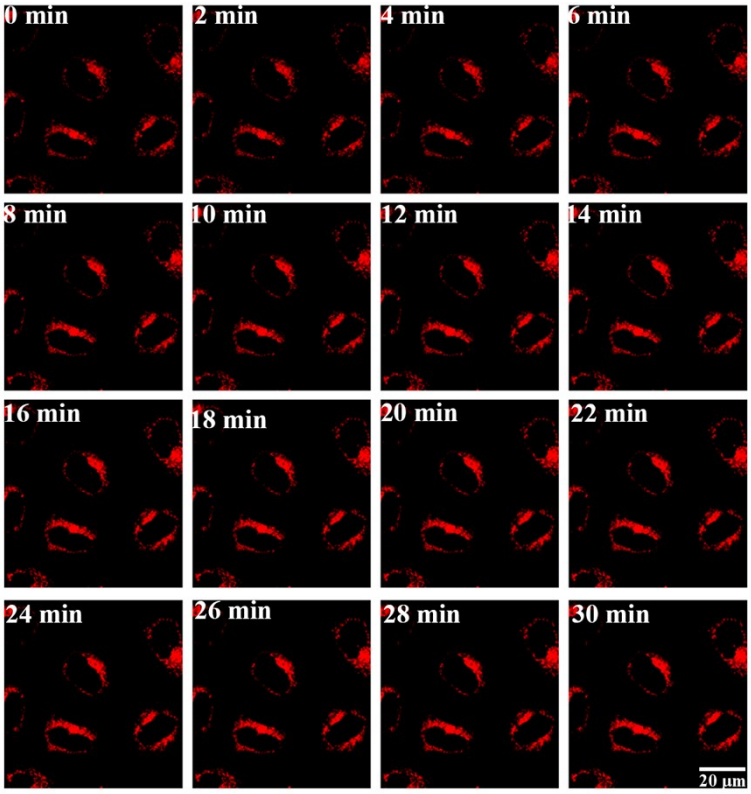

Figure S8. Dynamic fluorescent pictures HeLa cells co-incubated with **AF-Cy-2** after 30 min of irradiation at a constant temperature of 37 °C. Images were taken after co-incubated with **AF-Cy-2** (5 μM). Scale bar: 20 μm.

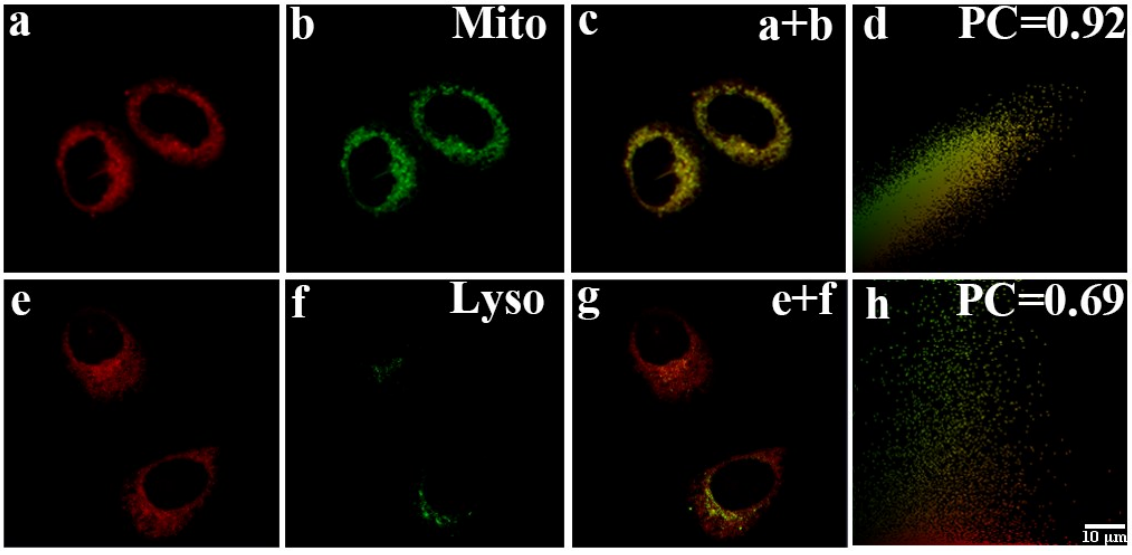

Figure S9. Confocal microscopic images of **AF-Cy-2** colocalized with commercially available organelle trackers in HeLa cells. HeLa cells were incubated with (a) **AF-Cy -2**(5.0 μM) for 0.5 h and then (b) with MitoTracker Green FM (0.05 μM), (c) Merged image of (a) and (b), (d) Colocalization scatterplots of (c); HeLa cells were incubated with (e) **AF-Cy-2** (5.0 μM) for 0.5 h and then (f) with Lysotracker Green (0.05 μM),

(g) Merged image of (e) and (f), (h) Colocalization scatterplots of (g). Scale bar: 10 μm.

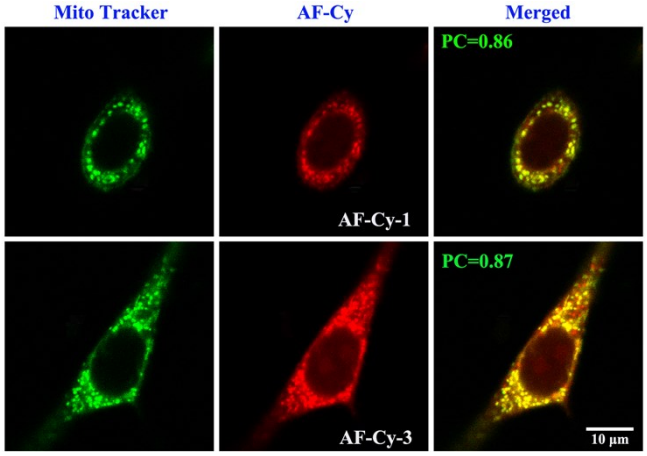

Figure S10. Confocal microscopic images of **AF-Cy-1** and **AF-Cy-3** colocalized with commercially available MitoTracker Green FM in 4T1 cells. Scale bar: 10 μm.

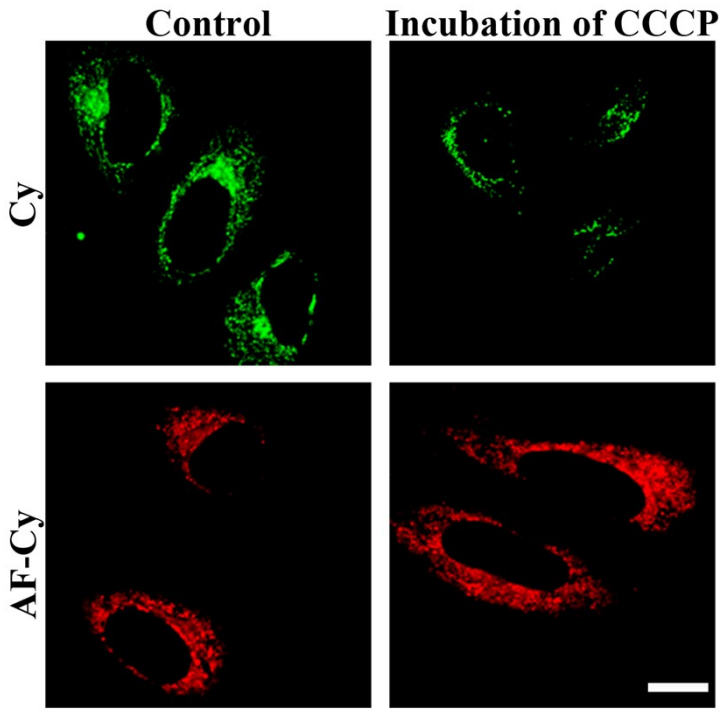

Figure S11. Analysis of **AF-Cy-2** immobilized in mitochondria of HeLa cells. The effect of CCCP, a recognized mitochondrial uncoupler, on the fluorescence confocal images of **AF-Cy-2** and the control **Cy** without aldehyde modification in HeLa cells. Scale bar: 20 μm.

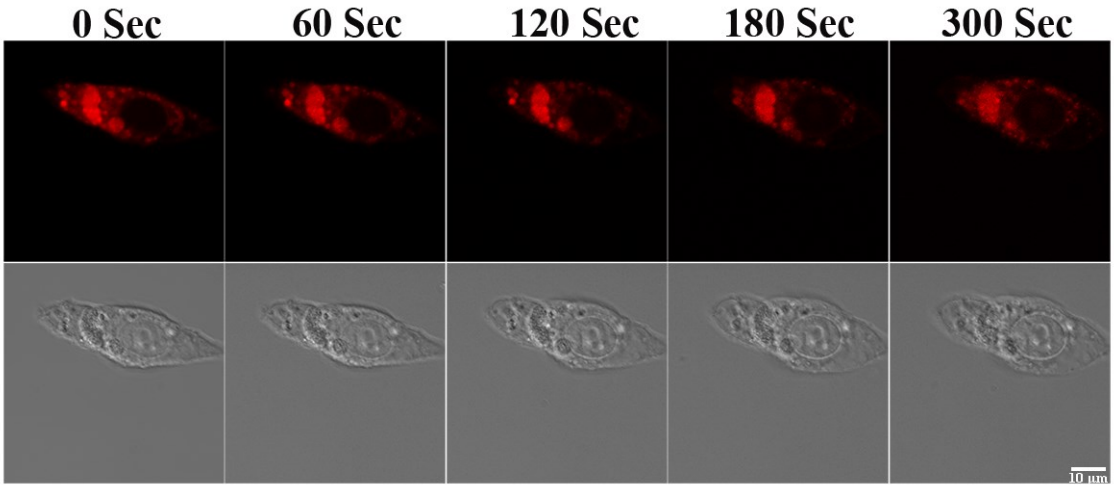

Figure S12. Analysis of **AF-Cy-2** immobilized in mitochondria of HeLa cells under the conditions of simulated photothermal treatment experiment (638nm laser continuous irradiation for 0-5 min, 1W / cm^2). Scale bar: 10 μm.

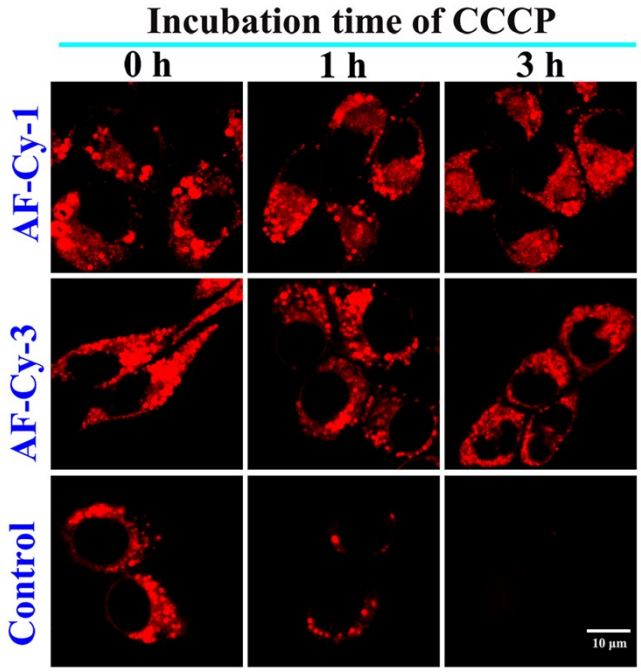

Figure S13. Analysis of the immobilized ability of **AF-Cy-1** and **AF-Cy-3** in mitochondria of 4T1 cells. Scale bar: 10 μm.

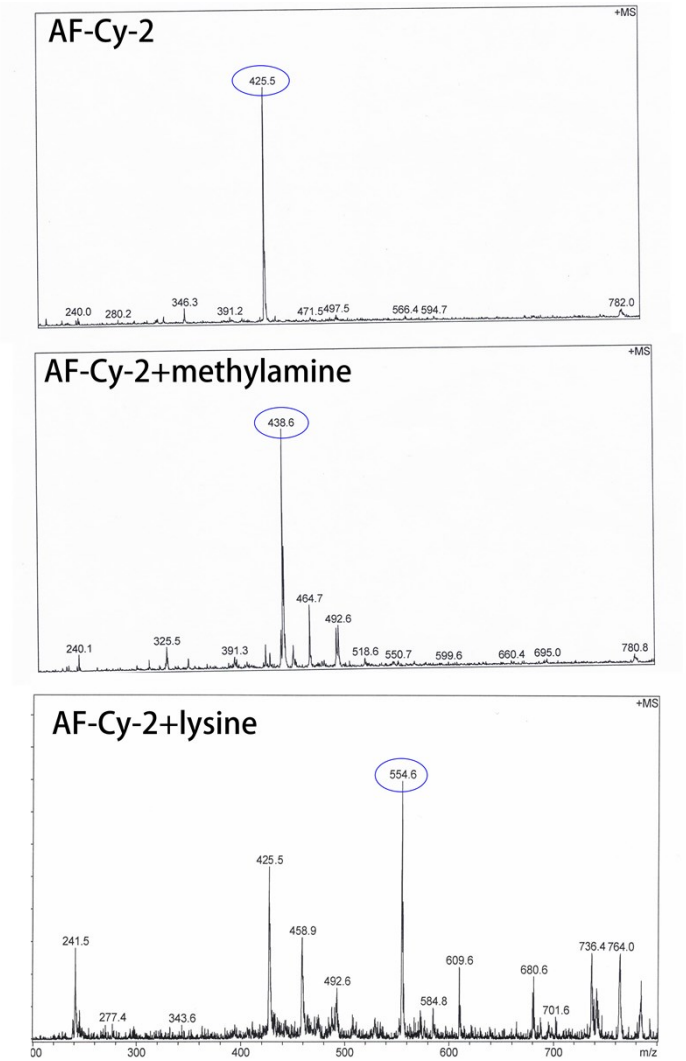

Figure S14. ESI-MS of **AF-Cy-2** reaction with methylamine or lysine.

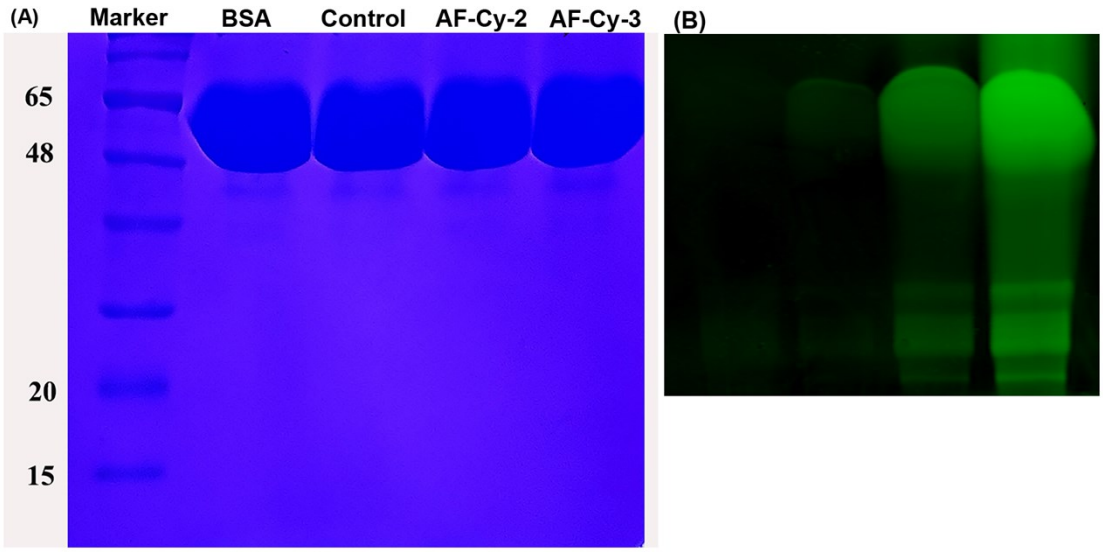

Figure S15. Analysis of **AF-Cy** immobilized on model protein. (A) PAGE of BSA

with **AF-Cy-2** and **AF-Cy-3**; (B)The corresponding fluorescence imaging pictures in Odyssey CLx system.

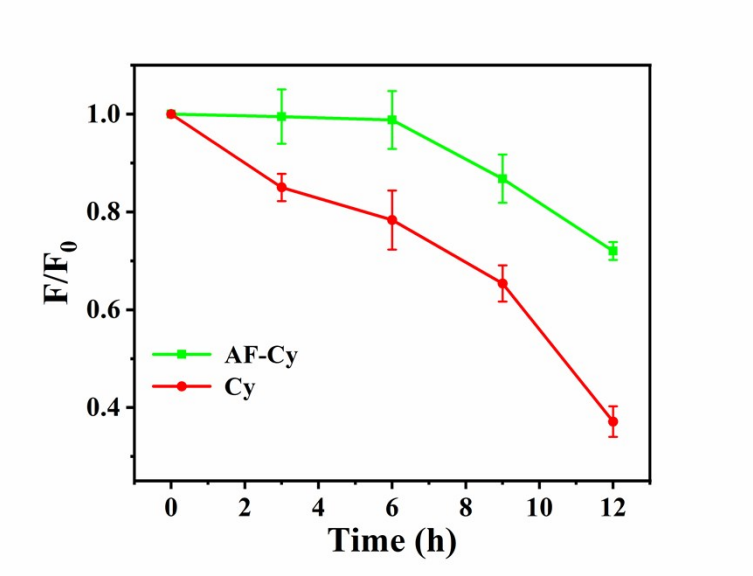

Figure S16. Quantification of fluorescence intensities of tumor as a function of post-injection time of **AF-Cy-2** (green line) and **Cy**(red line).

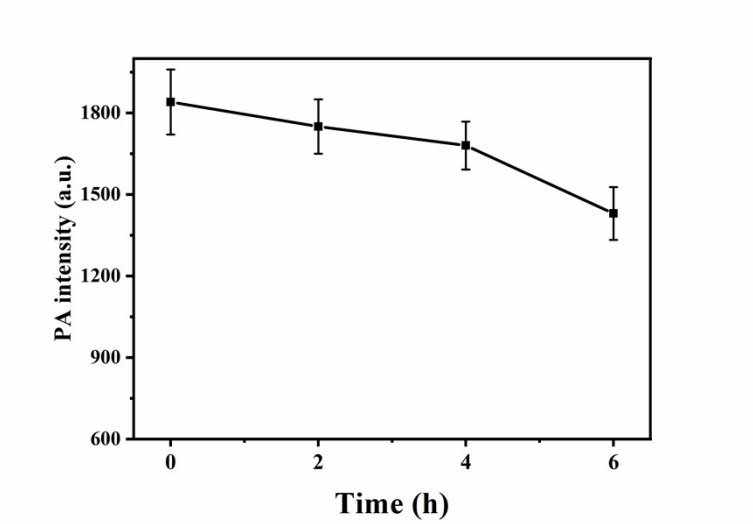

Figure S17. Quantification of photoacoustic intensities of tumor as a function of post-injection time of **AF-Cy**.

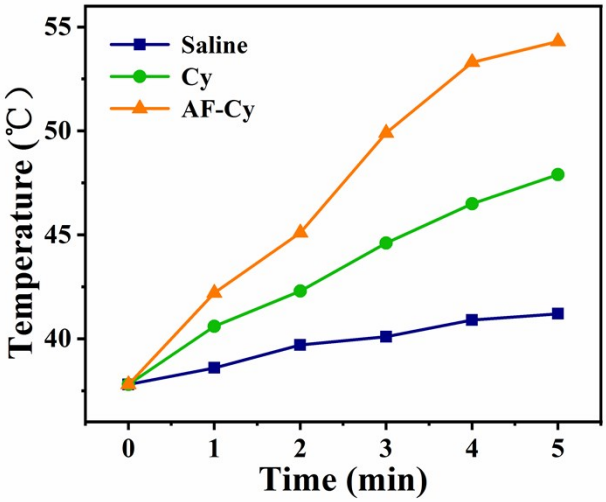

Figure S18. Mean tumor temperature during laser irradiation after post-injection of saline, **AF-Cy-2** or **Cy** (100 μM) into 4T1 tumor-bearing mice.

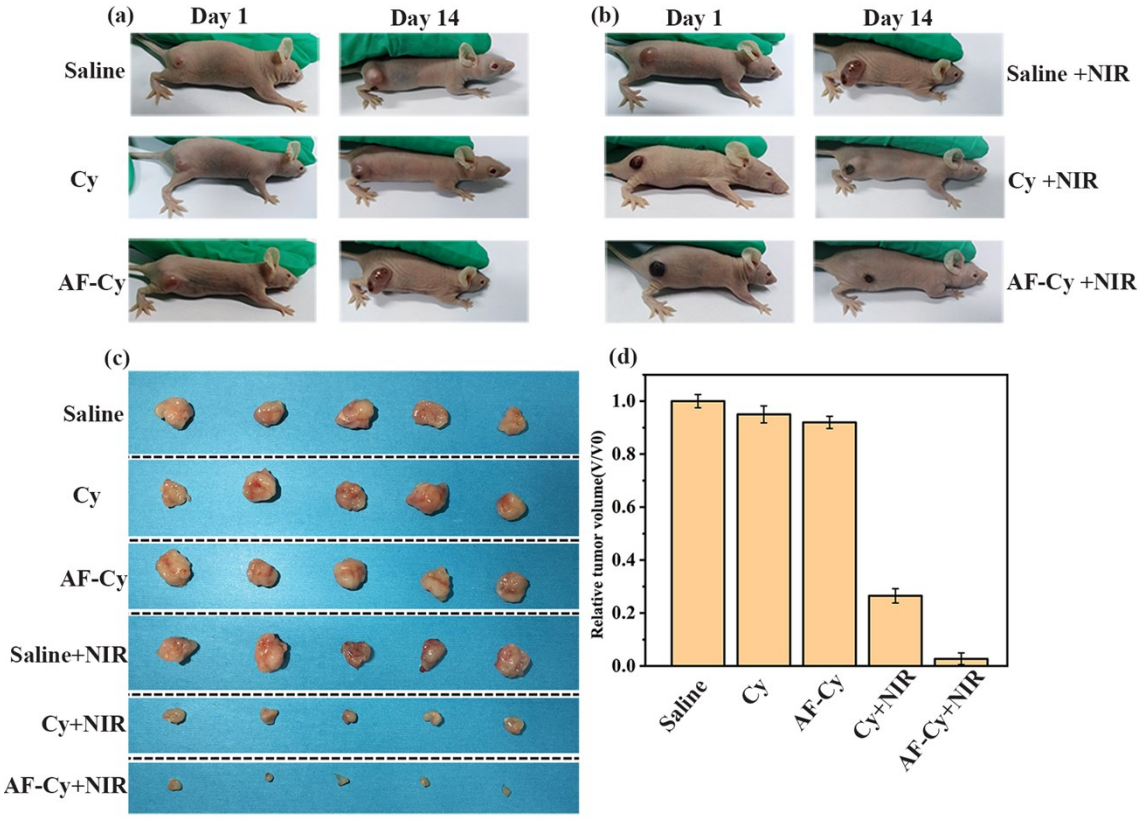

Figure S19. (a-b)Representative photographs of 4T1 tumor-bearing mice after different treatments; (c) Photographs of tumors size after different treatments; (d) Relative size of tumor after different treatments.

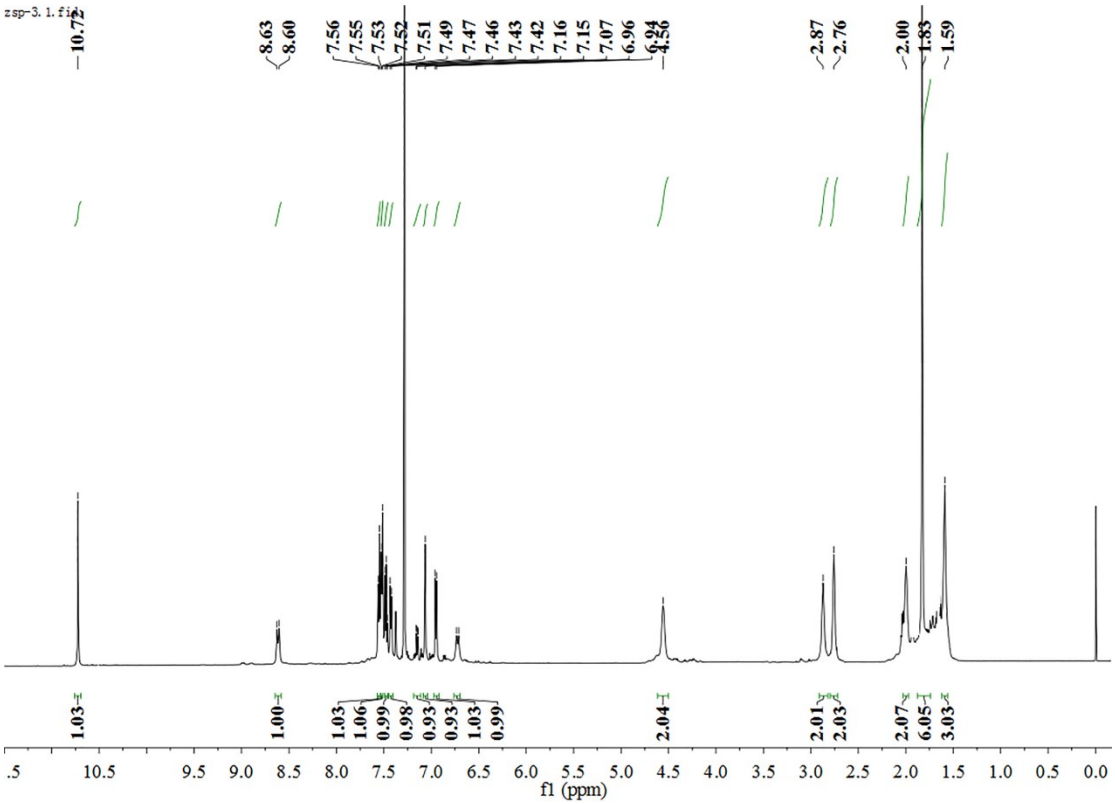

Figure S20. ^{1}H NMR spectrum of **AF-Cy-1** ($CDCl_3$).

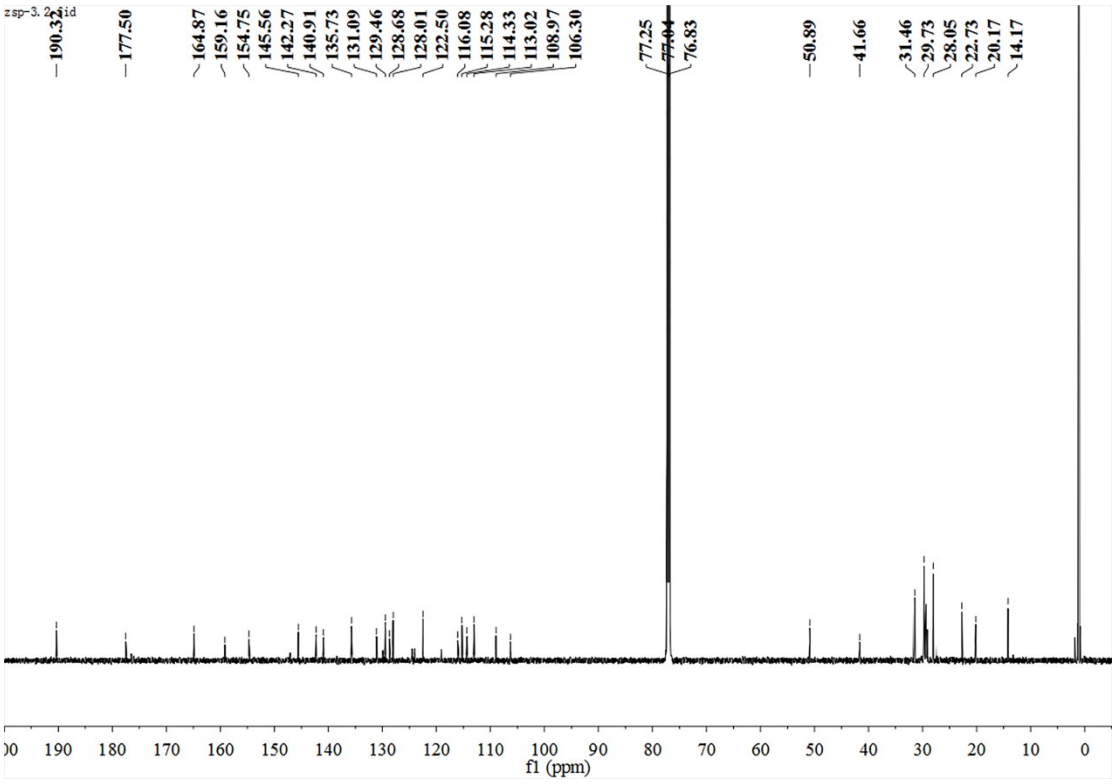

Figure S21. ^{13}C NMR spectrum of **AF-Cy-1** ($CDCl_3$).

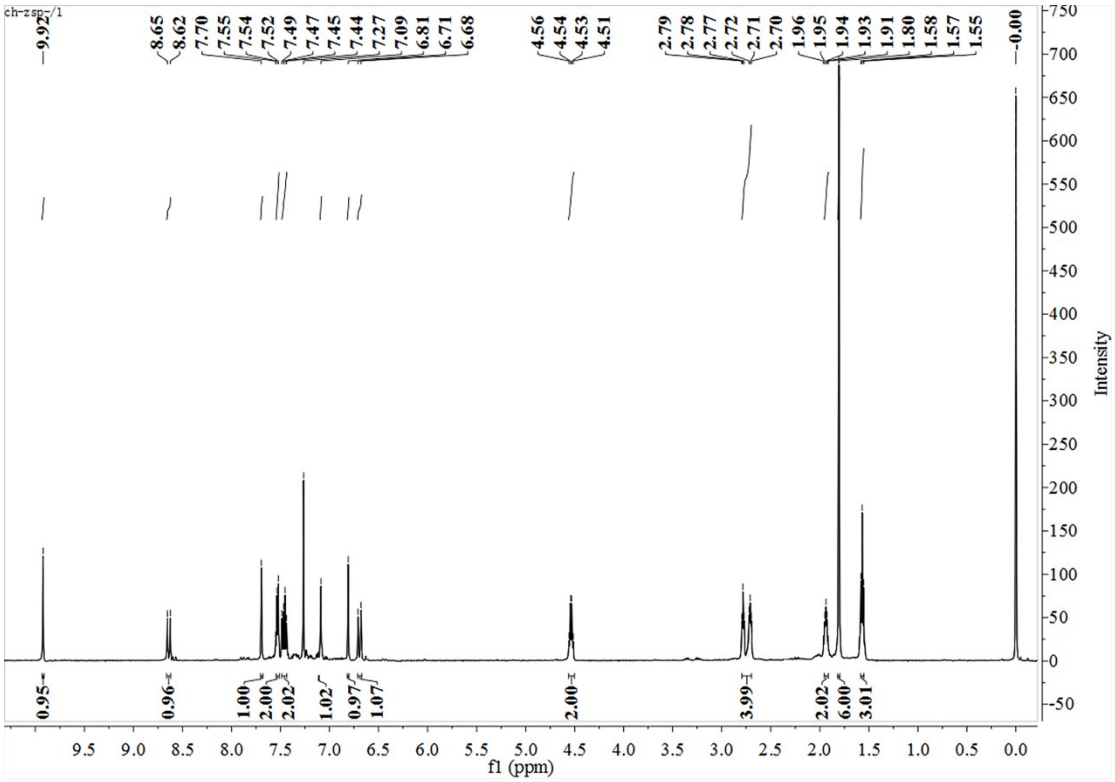

Figure S22. ^{1}H NMR spectrum of **AF-Cy-2** ($CDCl_3$).

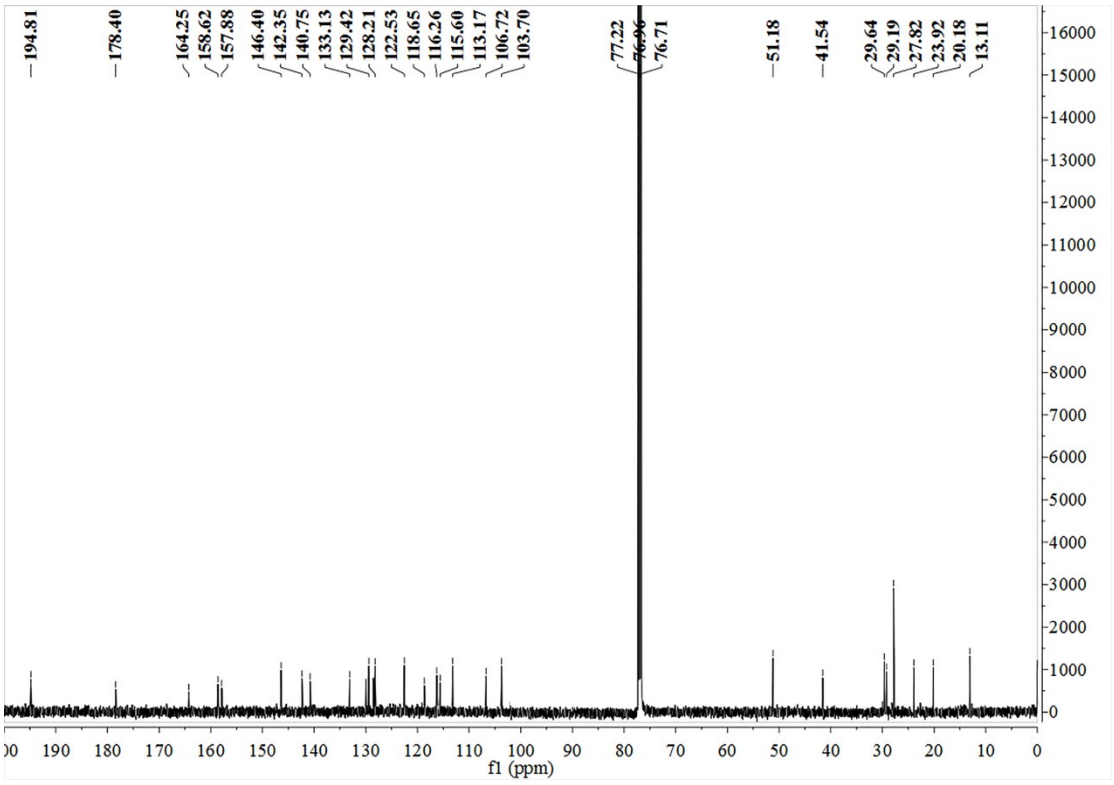

Figure S23. ^{13}C NMR spectrum of **AF-Cy-2** ($CDCl_3$).

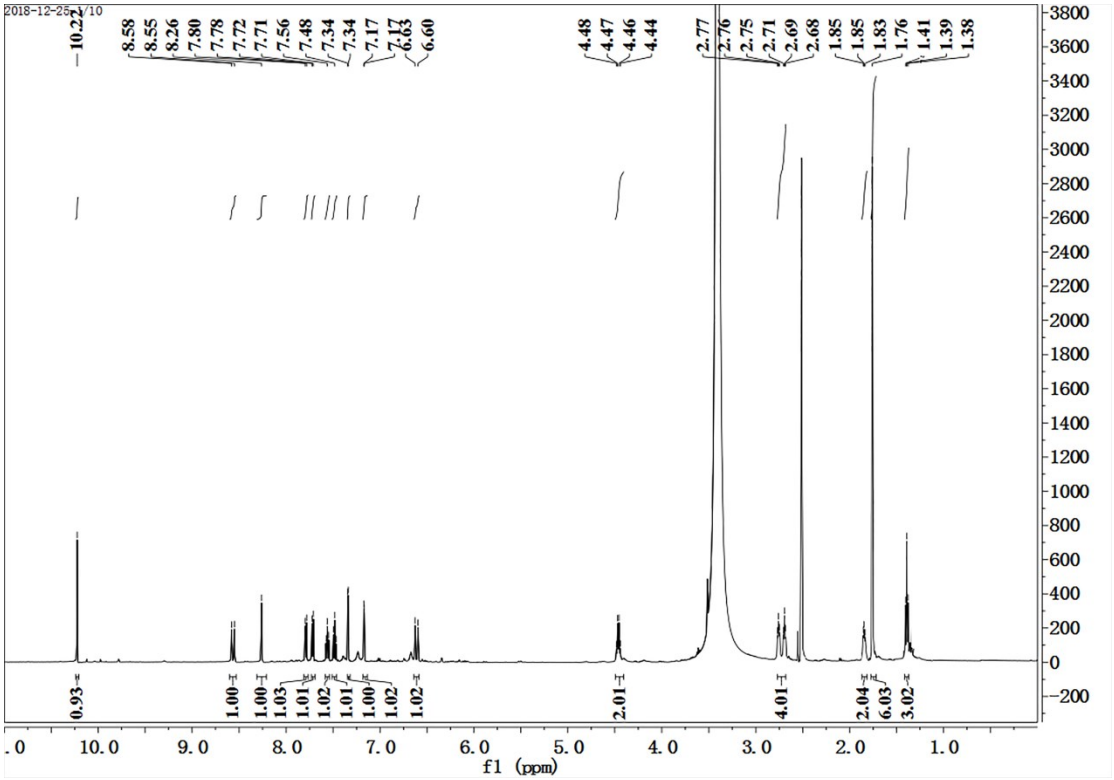

Figure S24. ^{1}H NMR spectrum of **AF-Cy-3** (DMSO-d_6).

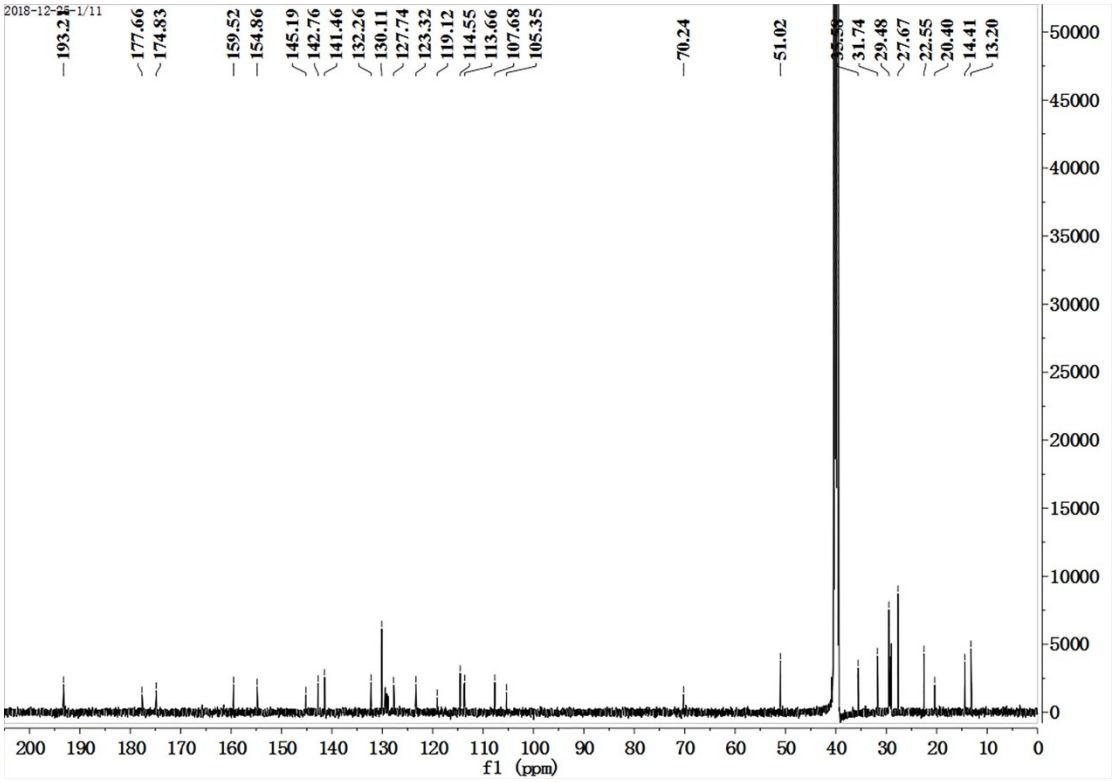

Figure S25. ^{13}C NMR spectrum of **AF-Cy-3** (DMSO-d_6).